

A directional DAS sensor and multi-component geophone comparison

Kevin W. Hall and Kris Innanen

ABSTRACT

Two surveys were acquired at the Containment and Monitoring Institute Field Research Station (CaMI.FRS) in 2018 that have common shots recorded on optical fibre (strain-rate; VSP and directional DAS surveys), geophones (velocity; VSP and directional DAS surveys), and accelerometers (acceleration; VSP survey only). Accelerometer data may be integrated to compare to geophone data, and we propose to further convert integrated accelerometer and unmodified geophone data to strain-rate by simply subtracting two traces, dividing by the distance between them, and plotting the result at a position halfway between the original traces.

INTRODUCTION

We wish to directly compare seismic data acquired on different sensors for a common shot, and in particular accelerometer and geophone data to DAS data. In order to do so, the data must be converted to a common domain, be that acceleration, velocity, strain rate, or strain. Accelerometer data with amplitudes that are proportional to the acceleration of the media the sensor is attached to may be converted to velocity by integration. Similarly, strain can be obtained by integrating strain-rate data. It is, perhaps, less obvious how to convert velocity data to strain rate. In this report, we propose a method of how to do this conversion and provide examples from two surveys that were acquired at the Containment and Monitoring Institute Field Research Station (CaMI.FRS) in 2018 (Figure 1).

VSP

A multi-azimuth walk-away vertical seismic profile (VSP) acquired at the CaMI.FRS is described in detail by Hall et al. (2018a, b, c), along with efforts that have been made to assign receiver geometry to fibre traces (Hall and Lawton, 2018, 2019). This report will concentrate on a single vibe point (VP 4151) from the VSP which is located approximately 24 m from observation well 2 (OBS2; Figure 1). The VSP was acquired with 2 sweeps per VP using a 1-160 Hz linear sweep using and Inova UniVib. Recording systems and receivers were as follows; 1) A Geode recording system listening to OYO GS-32CT 10 Hz 3C geophones at a nominal 5 m spacing in OBS2, 2) An Inova Scorpion recorder (High Definition Seismic Corporation) listening to VectorSeis accelerometers at a nominal 1 m spacing in OBS2, and 3) A Fotech distributed acoustic sensing (DAS) interrogator attached to the CaMI.FRS fibre loop sampling at 0.6667 m and using a 10 m gauge length. See Hall and Lawton (2019) for a detailed description of the borehole geometry.

Directional DAS sensor

Four additional vibe points (VP1-VP4; Figure 1) were acquired on a directional DAS sensor that is described in detail by Innanen et al. (2018). These VP were acquired with 10 sweeps per vibe point with a 10-160 Hz sweep run on the University of Calgary's IVI EnviroVibe. The directional DAS sensor was constructed using the same straight and

helical fibre that is found in the 1 km trench in the CaMI.FRS fibre loop and consists of two squares (eight 10 m long segments) that are repeated twice for each kind of fibre. The fibre is buried approximately 2 m below the surface. DAS data on the directional sensor were acquired using a Halliburton interrogator sampling at 1.0254 m with a 5 m gauge length. Nine Inova SM7 3C 10 Hz geophones and Inova Hawk recorders were placed around the direction DAS sensor, with eight geophones at the corners planted in undisturbed ground and one in the centre (Figure 1). Geophone pairs parallel to fibre segments are nominally 11 m apart.

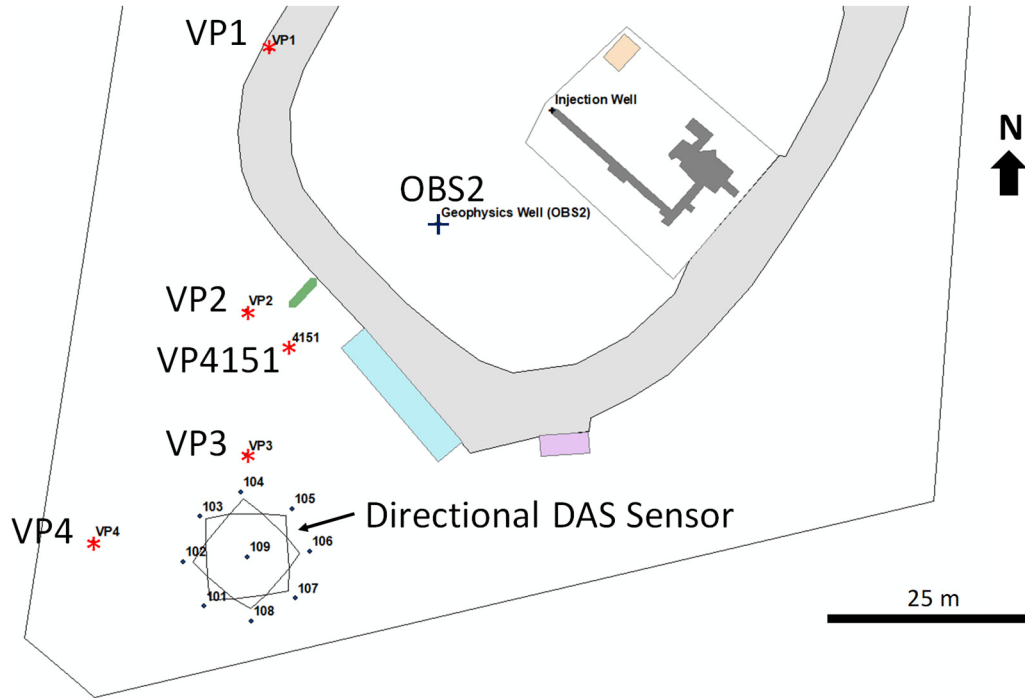


FIG. 1. Map showing VP and receiver locations for this report. VP 4151 was recorded on accelerometers, geophones, straight fibre and helically wound fibre in observation well 2 (OBS2). VP 1-4 were recorded on an experimental directional DAS sensor in addition to 3C geophones.

METHOD

In a one-dimensional sense, strain rate can be thought of as the velocity at which the two ends of a rod are moving towards or away from each other divided by the length of the rod. In the seismic case, geophones at two different locations measure the velocity of ground motion at those locations. So, to convert velocity information at two points on the ground to a strain-rate we propose to use the following equation,

$$\dot{\epsilon}_{xx} = \frac{\partial \dot{u}_x}{\partial x} \approx \frac{\dot{u}_x(x_2) - \dot{u}_x(x_1)}{\Delta x}, \quad (1)$$

where $\dot{\epsilon}_{xx}$ is the strain rate over some reference distance along the media (Δx), and $\dot{u}_x(x)$ represents velocity data (geophone data or integrated accelerometer data) recorded at position x (eg. Figure 2). The resulting strain-rate trace should then be plotted at position $\Delta x/2$ for comparison to fibre data. In practice, since we are dealing with proportions and the data in this report is displayed with individual trace scaling it is possible to skip dividing

our subtraction result by Δx . It is not clear how we could easily reverse this process to obtain velocity from strain rate.

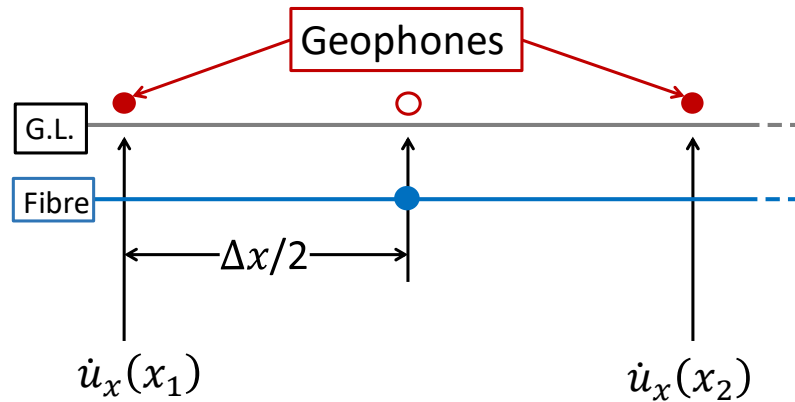


FIG. 2. Geometry of parameters used to calculate strain rate from geophone data for the directional DAS sensor.

EXAMPLES

VSP

Figure 3 shows VSP data for VP 4151 acquired in OBS2 plotted to the left of its average amplitude spectrum (blue). As fibre data records strain-rate along the axis of the fibre, we are choosing to compare the fibre data to the vertical component geophone and accelerometer data. While we expect the geophone and fibre data to have the same inclination in the borehole, which is not truly vertical (Hall and Lawton, 2019), the accelerometer data was corrected to true vertical in the field. The vertical component data has not been rotated to account for the VP offset of 24 m from the well. Accelerometer and fibre data have been windowed in depth and time to match the geophone display. In general, the helically wound fibre data is lower amplitude and noisier than the straight fibre data but is comparable after trace scaling for display.

Breaks in slope visible in the direct arrivals of the geophone and accelerometer data are due to the removal of dead traces. Note that this type of display has one trace per column, so the depth scale across the bottom is approximate. Horizontal bands of noise on the fibre data are likely due to internal coupling within the interrogator, which was quite close to the vibe point. Noise increases as the Vibe approaches junction boxes where the fibre exits the ground to electrical boxes to the point that the 24 m offset VP was judged to be the closest usable to the well for these figures.

Integration and a high pass filter to exclude integration noise below 1 Hz performed on the accelerometer data results in the updated Figure4. This step has resulted in a very good match in the accelerometer and geophone amplitude spectra above 10 Hz. Visually, the source gathers are also a much better match.

Conversion of geophone and integrated accelerometer data to strain rate using Equation 3 gives us the results shown in Figure 5. The amplitude spectra now more closely match the fibre data but are not an exact match. Visually, the phase of the up-going wavefield is

now a better match than that seen in Figure 4. The geophone and accelerometer data appear to have higher frequency content than the fibre data. It would be interesting to see how deconvolution changes this observation.

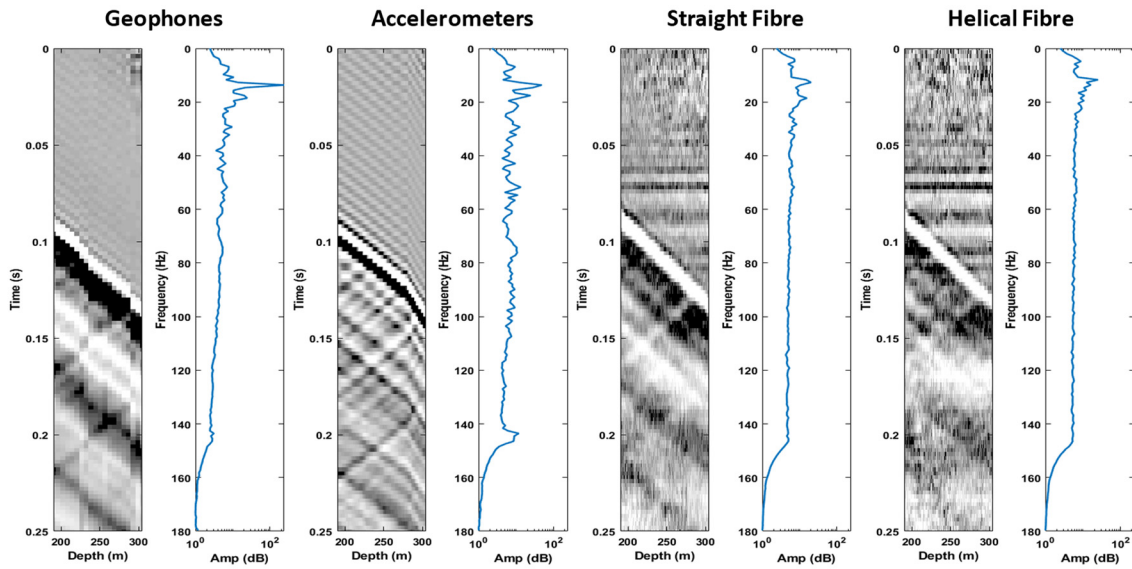


FIG. 3. Data from VP 4151 recorded on downhole sensors in observation well 2 (OBS2).

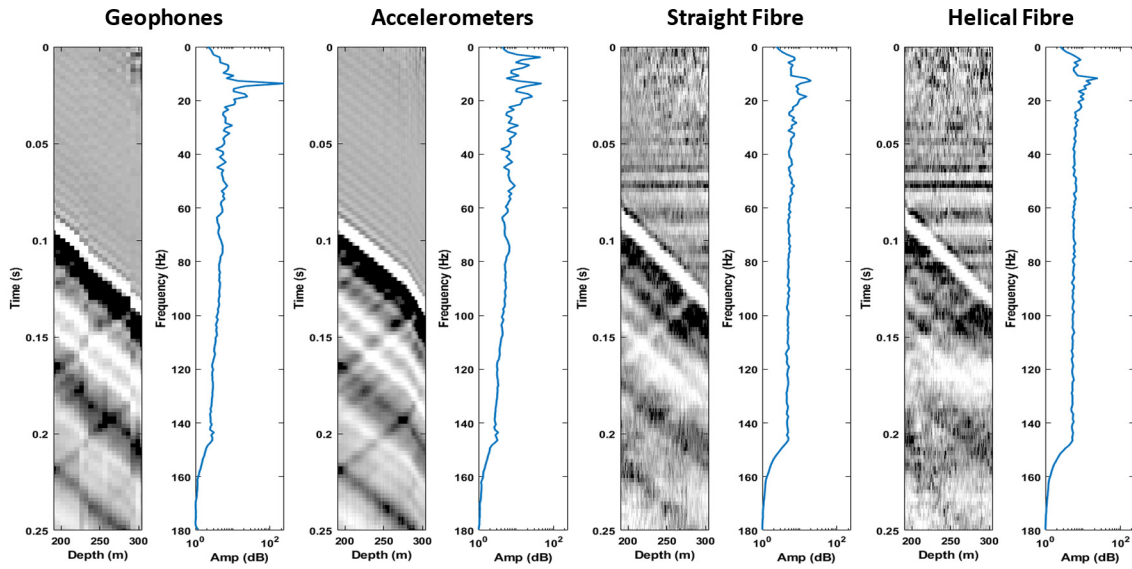


FIG. 4. Data from VP 4151 recorded on downhole sensors in observation well 2 (OBS2), after integrating the Accelerometer data.

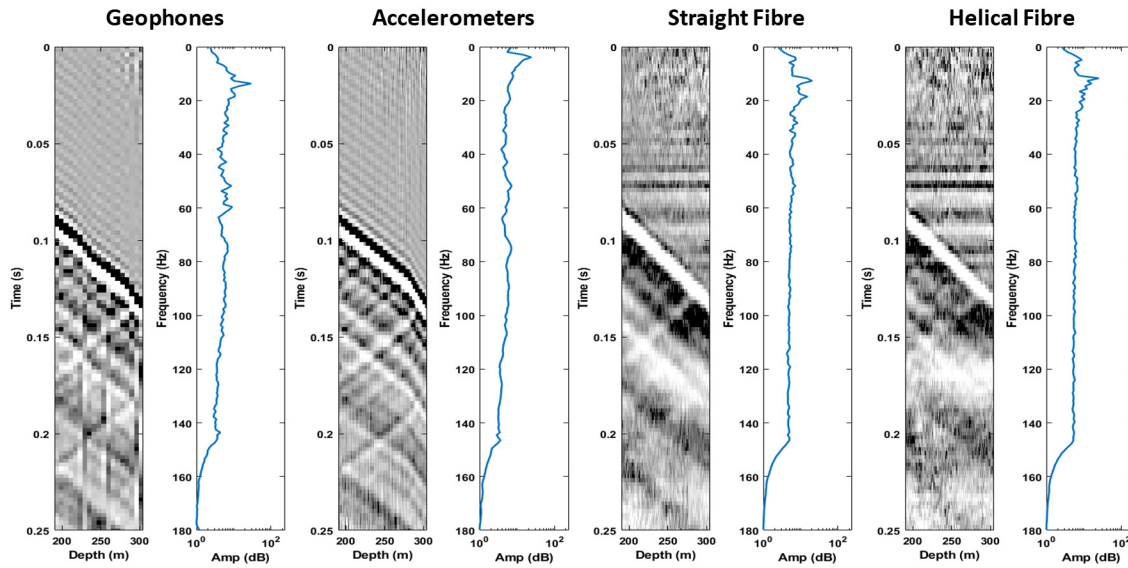


FIG. 5. Data from VP 4151 recorded on downhole sensors in observation well 2 (OBS2), after converting accelerometer and geophone data to strain rate.

Directional DAS sensor

To convert 3C geophone data to strain rate for the directional DAS sensor, it makes sense to use the horizontal geophone components after component rotation to inline with a given fibre segment (Figure 6). Black arrows show the orientation of geophone horizontal components (oriented to magnetic north). Blue arrows (inline with fibre segment) and Magenta arrows (crossline to fibre segment) show component orientation after rotation.

Without doing any trace interpolations, the location of each fibre segment in the directional sensor was interpreted from the fibre data by comparison to synthetics (cf. Innanen et al., 2018) and using a trace spacing of 1.0 m for straight fibre and 0.866 m for the helical fibre. Halfway positions on fibre segments were then found by shifting a half segment length (~ 5 m). This process could be optimized in future, but for a first try is likely good enough. Note that the fibre data appear to have an approximately 100 ms delay in time from the geophone data. We have chosen to assume that this time delay is exactly 100 ms, and bulk-shifted the fibre data accordingly.

Given that 1) geophones on the surface were exposed to air blast and wind noise unlike the buried fibre, and 2) the geophones were not exactly coincident with fibre locations projected to the surface, the unfiltered conversion to strain rate results for VP 1-4 look remarkably like the fibre data (Figures 7-12). Peaks in the red graph along the bottom of these figures highlight the location of geophone traces.

It may be possible to improve the match via better determination of the time-delay, filtering, and trace-balancing. Our best results are for VP1, so Figure 11 shows a close-up of the data for straight fibre wrapped around square 1 (segments 1-4), and Figure 12 shows the corresponding amplitude spectra.

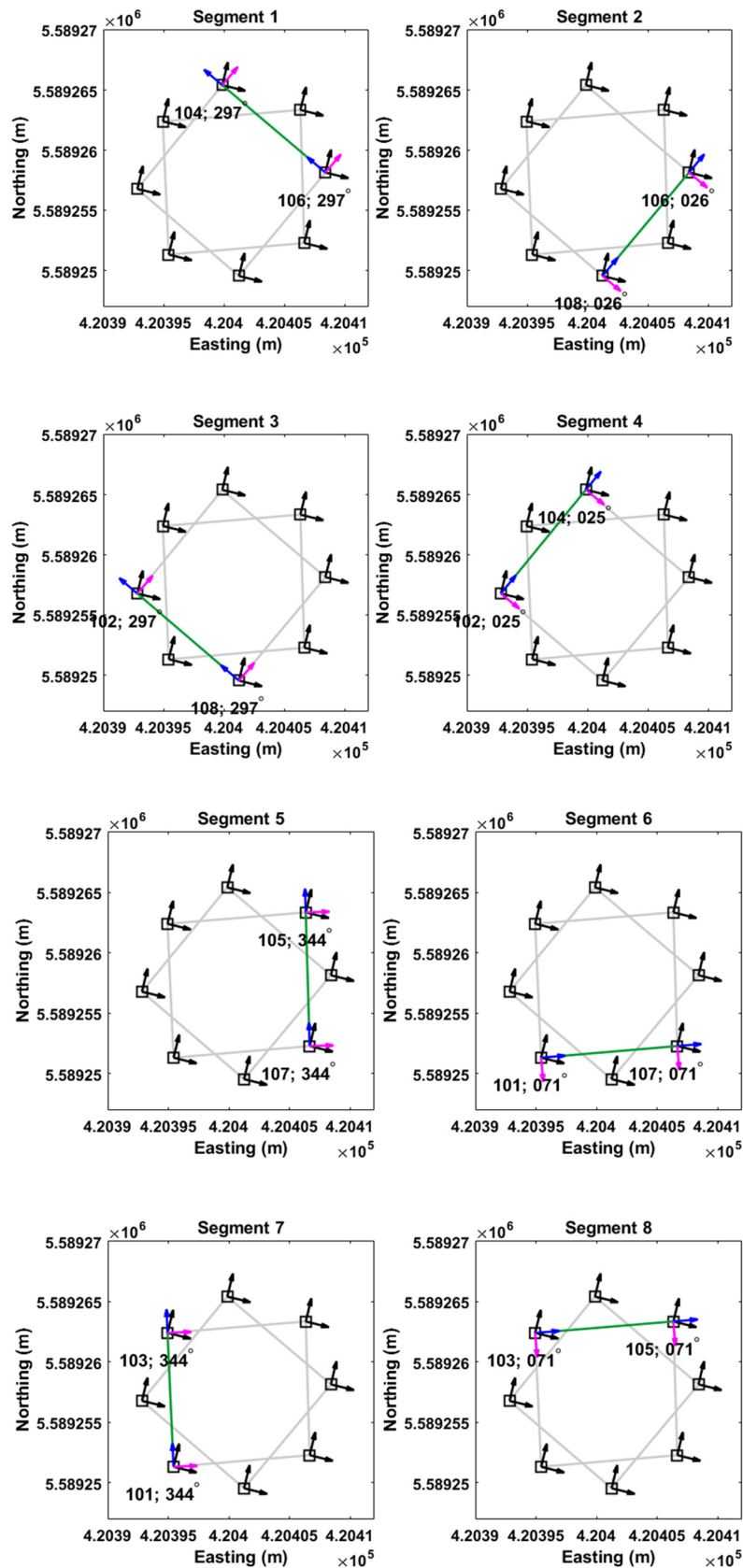


FIG. 6. Examples of 3C geophone component rotations for four each of the eight segments.

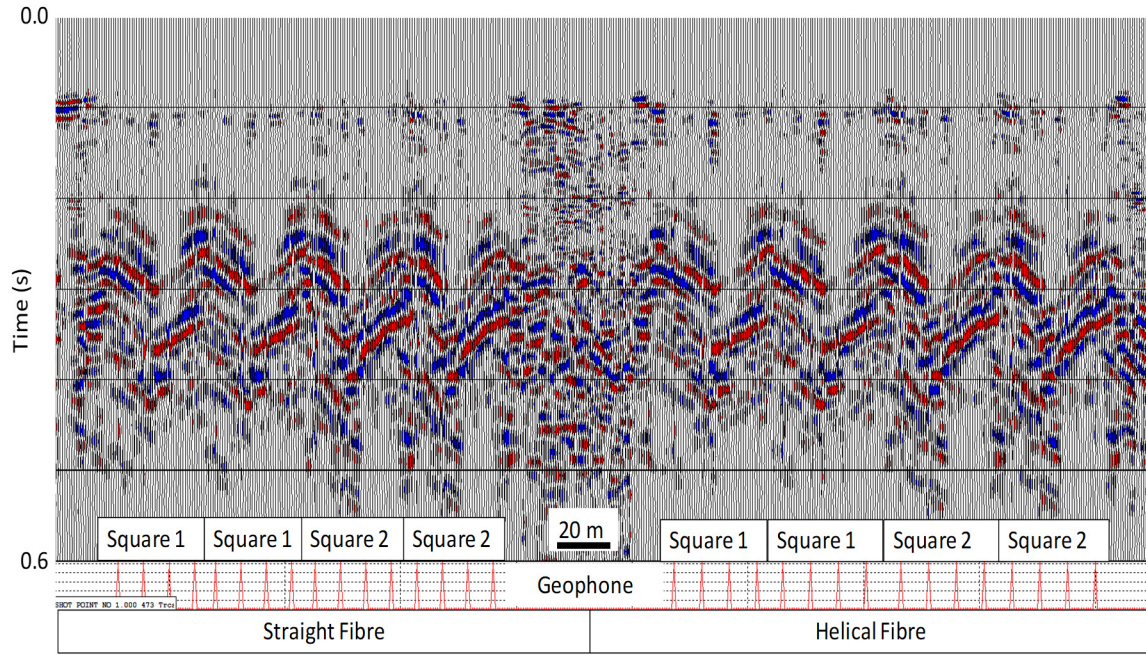


FIG. 7. VP 1; Geophone data converted to strain rate and interleaved with straight and helical fibre data. Peaks in the red graph along the bottom highlight the location of geophone traces.

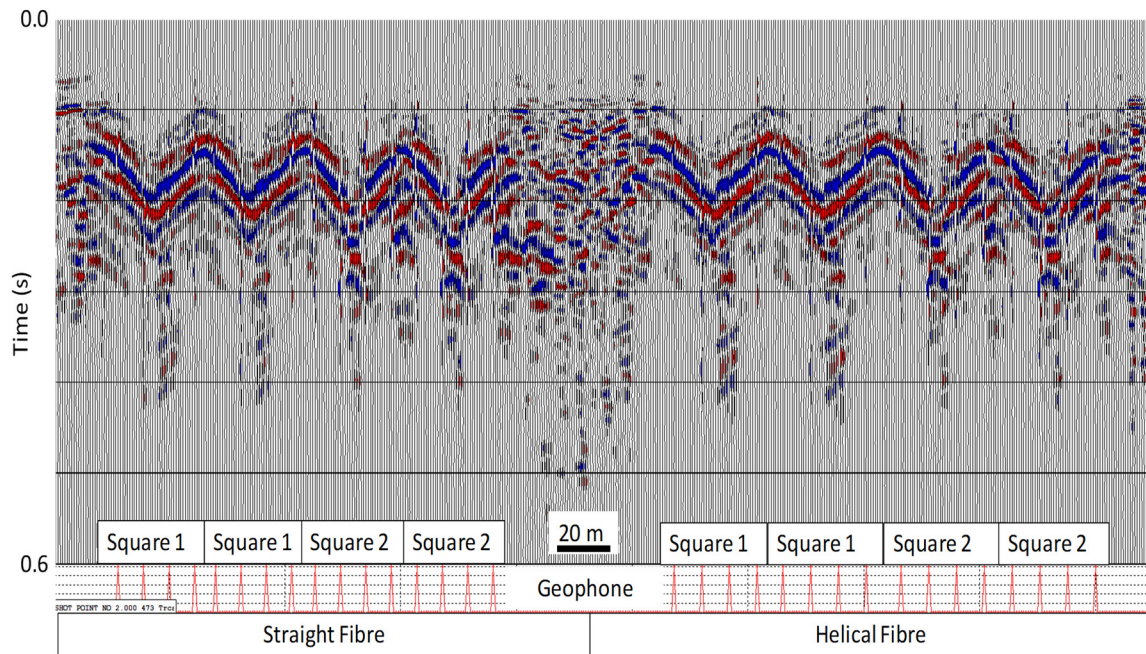


FIG. 8. VP 2; Geophone data converted to strain rate and interleaved with straight and helical fibre data. Peaks in the red graph along the bottom highlight the location of geophone traces.

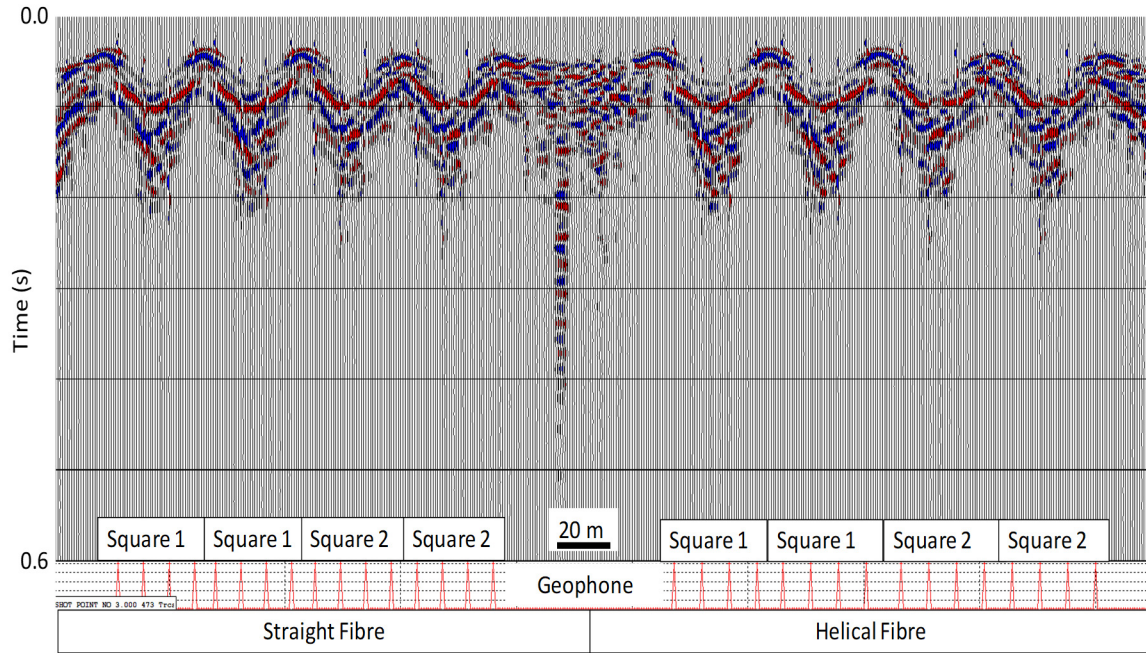


FIG. 9. VP 3; Geophone data converted to strain rate and interleaved with straight and helical fibre data. Peaks in the red graph along the bottom highlight the location of geophone traces.

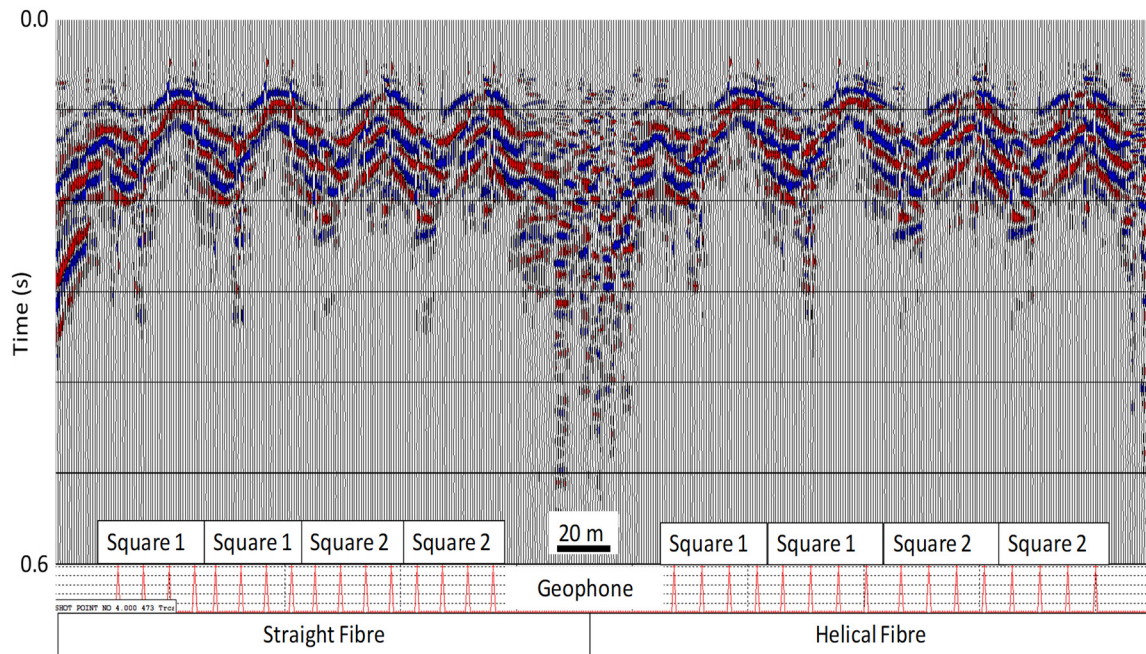


FIG. 10. VP 4; Geophone data converted to strain rate and interleaved with straight and helical fibre data. Peaks in the red graph along the bottom highlight the location of geophone traces.

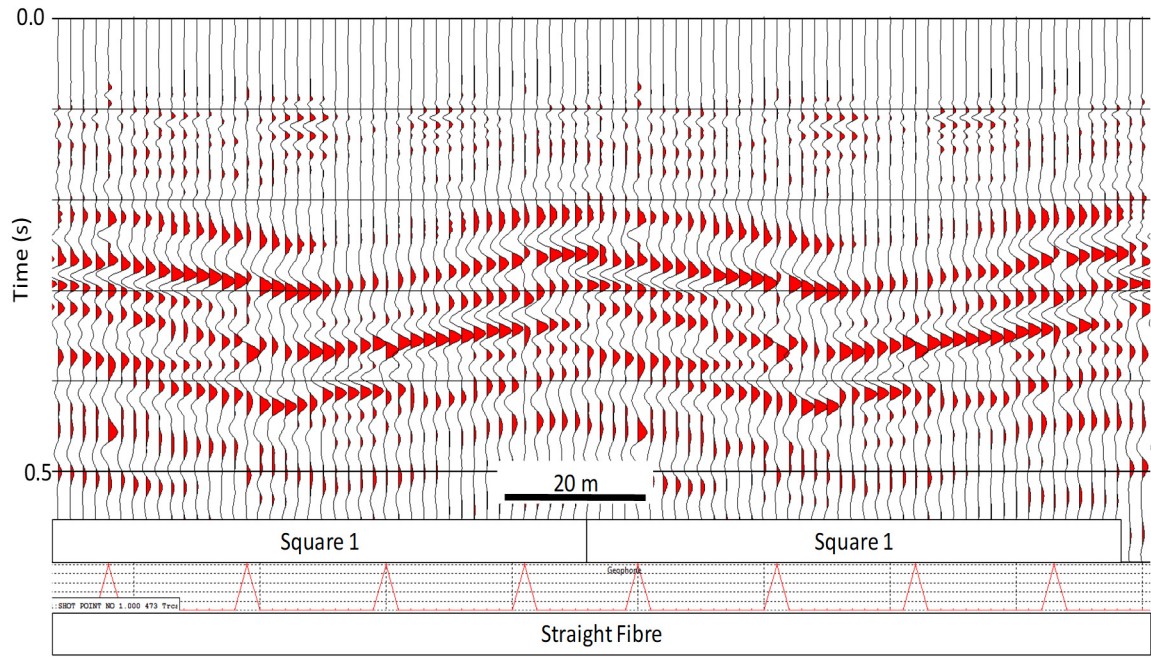


FIG. 11. VP1; Close-up of geophone data converted to strain rate and interleaved with straight fibre data. Peaks in the red graph along the bottom highlight the location of geophone traces.

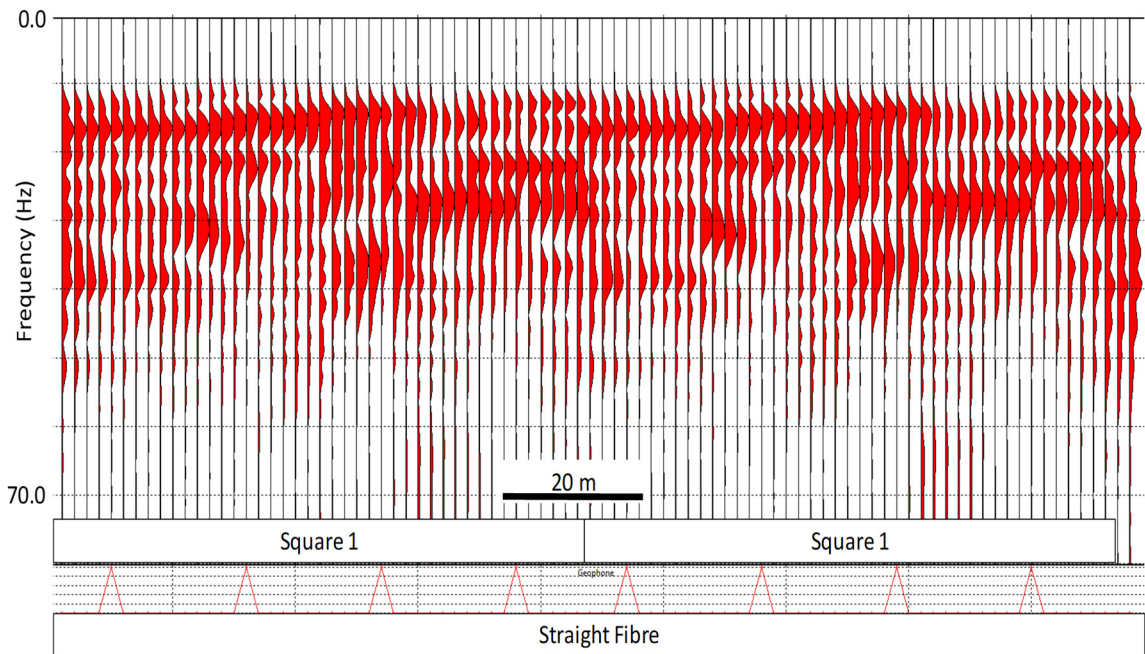


FIG. 12. VP1; Amplitude spectra for traces shown in Figure 11.

DISCUSSION

A method to convert seismic data with amplitudes proportional to particle velocity to strain rate for comparison to distributed acoustic sensing (DAS) fibre data has been proposed and some initial testing has been carried out on surface and borehole data acquired at the CaMI.FRS. Results for both datasets are encouraging, and we feel that further work is warranted.

ACKNOWLEDGEMENTS

The authors would like to thank Fotech, Halliburton, Lawrence Berkeley National Laboratory. We would also like to thank Schlumberger for the use of donated Vista software, and all CREWES sponsors and CaMI.FRS JPI subscribers for continued support. This work has been partially funded by NSERC (Natural Science and Engineering Research Council of Canada) through the grant CRDPJ 461179-13. This research was also supported in part by the Canada First Research Excellence Fund.

REFERENCES

- Hall, K.W., Bertram, K.L., Bertram, M., Innanen, K., and Lawton, D.C., 2018, CREWES 2018 multi-azimuth walk-away VSP field experiment: CREWES Research Report 16, 30.
- Hall, K.W., and Lawton, D.C., 2018 Optical fibre data registration: CREWES Research Report 17, 30.
- Hall, K.W., and Lawton D.C., 2019, DAS trace location assignment for the CaMI.FRS Fibre loop: CREWES Research Report, This volume.
- Innanen, K., Lawton, D.C., Hall, K.W., Bertram, K.L., Bertram, M. and Bland, H., 2018, Design and deployment of a prototype multicomponent DAS sensor: CREWES Research Report 23, 30.